

Flow Structure in the Near-Wall Zone of a Turbulent Separated Flow

E. W. Adams* and J. P. Johnston†
Stanford University, Stanford, California

The flow and turbulence structure in a thin reversed flow layer under a recirculation zone was investigated for the case of a turbulent reattaching flow behind a backward-facing step. The step-height Reynolds number was 36,000, and the separating boundary layer was fully turbulent ($Re_\theta = 3700$). A number of techniques, including hot-wire anemometry and laser-Doppler anemometry, were used. Results include U and u' profiles, wall shear stresses by the pulsed wall probe method, and frequency spectra. These data and other related studies^{6,15} suggest that the shear stress throughout the layer is predominantly viscous, even though the fluctuation levels are very high. Despite the high levels of fluctuation, the flow appears to be "laminar-like"¹² from the wall out to the region of maximum local backflow velocity.

Introduction

THE study of turbulent separated flows has a long history because of its practical importance in many applications. The first detailed studies entailed measurements of the wall-pressure distribution,¹ flow visualization within the separation zone,² or the study of the "outer flow" around a separation bubble.³⁻⁵ With the inventions of the Laser Doppler Anemometer (LDA) and the Pulsed Wire Anemometer (PWA), which allow accurate measurement of the velocity field inside a region of turbulent separated flow, the amount of information on separated flows has grown rapidly, but due to the small thickness of the wall layer compared to overall thickness of the separated region, near-wall regions have received relatively little attention. (The near-wall region is defined as the layer of fluid flowing in the reversed direction between the solid surface and the maximum reversed velocity. The maximum reversed velocity U_N is the edge velocity for the shear layer of thickness N that forms the near-wall region. The flow above the near-wall region is not a freestream in the conventional sense.) Notable exceptions are the work of Simpson et al.,⁶ Westphal (in Simpson⁷), Devenport,⁸ and Ruderich and Fernholz.⁹ Skin-friction measurements, by methods thought to be independent of the validity of the log-law, have also been performed in reattaching flows.¹⁰⁻¹² It is the combination of near-wall velocity measurements with data on the wall shear stresses that allows the structure of the near-wall region to be evaluated; in particular, the applicability of the log-law may be examined. A realistic physical model of the very-near-wall region in a turbulent separated flow is a necessary condition for the adequate computation/prediction of the details of a region of separated and/or reattaching flow.

The existing evidence on the near-wall structure of separated flows suggests that this region is not a "normal" turbulent boundary layer (TBL). First, measured values of C_f in the recirculating region of backward-facing step flows, normalized on $\frac{1}{2} \rho U_N^2$, are typically¹²⁻¹⁴ on the order of 0.02, values that seem much too high for a TBL flow. Second, measured turbulent kinetic energy (TKE) balances from

Simpson et al.⁶ and Pronchick and Kline¹⁵ show that, beneath a separated zone in the near-wall region, turbulence dissipation largely balances turbulence diffusion, not turbulence production. Turbulence production is small, and neither set of data contains any region in the near-wall zone where production is even approximately equal to dissipation. Third, experimenters who have measured $-u'v'$ using two-component LDA systems in the near-wall region or even close to it show that $-u'v'$ is small. In this region, the magnitude of $-u'v'$ is less than the uncertainty of the data (see Refs. 6, 10, 15, and 16). If the near-wall region of separated flows is indeed turbulent, with a structure at all like that of a regular wall-bounded TBL, relatively large (measurable) values of $-u'v'$ would be expected. Without large correlated $-u'v'$, normal turbulent boundary-layer structure cannot exist.

The model of the near-wall flow structure presented here is based on detailed measurements in the turbulent separation bubble behind a backward-facing step. First, the model is developed by combining data on wall shear stress with those of mean velocity and streamwise turbulence intensity. The present data, like those of Ruderich and Fernholz⁹ and Devenport,⁸ show that a log-law region does not exist in the wall layer of a separated flow. Second, velocity measurements processed as frequency spectra are used to supply scale information for the near-wall flow. The complete array of data that results, combined with results from other investigators, suggests that the large turbulent fluctuations found very near the wall do not play a major role in the dynamics described by the equations of the mean motion. Thus, in some respects, the flow "looks" laminar if only the mean flow is examined. The velocity fluctuations scale, not on local variables, but on the global separation geometry. This suggests that their origin is in the free shear layer, not the wall layer. We agree with the terminology suggested by Castro and Haque.¹² The flow is laminar-like but not laminar in that it has large fluctuations superimposed.

Theoretical Background

The near-wall flow beneath a two-dimensional separation bubble is defined by the wall and a thickness $N(x)$ formed by the line connecting the locations of the maximum backflow velocity (Fig. 1). Because the flow in this region is characterized by large-velocity fluctuations, it is useful to decompose the velocity components into mean and fluctuating parts and then time-average the equations of motion, a procedure not limited to turbulent flows. It is a primary feature of turbulent shear flows, however, that the Reynolds stress terms play an

Received Sept. 14, 1987; presented as Paper 88-0610 at the AIAA 26th Aerospace Sciences Meeting, Reno, NV, Jan. 11-14, 1988. revision received Feb. 19, 1988. Copyright © American Institute of Aeronautics and Astronautics, Inc., 1988. All rights reserved.

*Research Assistant, Department of Mechanical Engineering; currently, Systems Engineer, United Research Center, East Hartford, CT.

†Professor, Department of Mechanical Engineering.

important, if not dominant, role compared to their laminar counterparts. If the flow in the near-wall layer, below the point of maximum reversed-flow velocity, is considered (Fig. 1), an order-of-magnitude analysis may be employed, following the typical arguments for thin shear layers. These arguments are valid in the near-wall region, if, as shown in Refs. 6 and 15, streamwise diffusion is a small fraction of cross-stream diffusion. The resulting equations, valid in the limit of $Re_x \gg 1$ and $N/x \ll 1$, are

$$\frac{\partial(\rho U^2)}{\partial x} + \frac{\partial(\rho UV)}{\partial y} = -\frac{\partial p}{\partial x} + \frac{\partial}{\partial y} \left(\mu \frac{\partial U}{\partial y} - \overline{u'v'} \right) + \frac{\partial}{\partial x} (u' - v')$$

$$\frac{\partial(\rho U)}{\partial x} + \frac{\partial(\rho V)}{\partial y} = 0$$

where x is the development distance of the reversed-flow shear layer. In the case of the backward-facing step, this is the distance upstream from the point of reattachment.

The equations themselves are unchanged from their boundary-layer form, but a uniform, nearly one-dimensional freestream no longer exists. The mean streamwise velocity profile has curvature, and the y gradient of the shear stress is finite at $y = N$, the location of the maximum reverse velocity U_N . Such a change in the outer boundary conditions should not change the structure of the inner region, but rather the positive curvature of the profile, caused by the positive shear gradient, will bow the reversed flow mean profiles, giving the appearance of a fuller profile, much like the effect created by freestream acceleration. Thus, when comparing the experimental results to existing normal solutions, it is expected that the experimental results will show a somewhat fuller profile shape.

Because the separated flow region studied here is a reattaching flow, the natural set of coordinates for studying the backflow zone has its origin at the reattachment point. All distances in the streamwise direction are normalized by the reattachment length $-X^* = (x_r - x)/x_r$, while distances in the cross-stream direction are normalized by the step height $Y = (y/H)$. Note that $-X^*$ increases with motion away from the reattachment point and toward the step. The minus sign is used to show explicitly that this is in the upstream direction when the motion of the entire flowfield is considered. For the near-wall region, $-X^*$ is the local mean flow direction. Westphal,¹¹ using mean velocity profiles, showed that data from various backstep experiments tend to collapse when plotted using X^* coordinates. This is also shown in the present wall shear stress results.

Experiment

The present series of experiments was performed using a multipurpose, low-speed, open-circuit wind tunnel.¹⁷ Flow conditioning, which included five screens and a 4:1 contraction-ratio nozzle, produced a uniform two-dimensional flow and a freestream turbulence intensity of 0.3% at the test section entrance. The experimental geometry used for generating the separation was a backward-facing step with an expansion ratio of 1:25 (Fig. 1). The spanwise aspect ratio of the wind tunnel was 11.4:1 based on step height, larger than the 10:1 aspect ratio criterion of Brederode and Bradshaw¹⁸ for the assurance of two-dimensional flow. All measurements were taken on the channel's spanwise centerline.

The step-height Reynolds number ($Re_H = HU_{ref}/\nu$) was 36,000 (U_{ref} is measured ahead of the step in the freestream). The boundary layer at the step edge was thick and turbulent ($\delta/H = 1.0$), with a momentum-thickness Reynolds number of 3700. In this configuration, the reattachment location X_r/H , as measured by two methods, the thermal tuft¹⁴ and the LDA, was 6.4.

As a preliminary to the present study, a detailed one-component LDA study of the experimental flow was performed. These results, reported in Ref. 19, confirmed the expected two-dimensionality of the test section flow, mass, and momentum balanced in the two-dimensional sense (see Ref. 20) to within 3%. The mean field data were also used to identify the near-wall region of $0.3 < -X^* < 0.67$ as a region of nearly complete backflow. That is, flow in this region, below the overriding separated shear layer, is moving in the upstream direction close to 100% of the time. In such a region, the signals from hot wires are not ambiguous, and thus, a special wall-mounted hot-wire probe was used to obtain information on the high-frequency velocity fluctuation, unavailable from the LDA, as well as to measure velocity profiles very close to the wall, out of reach of the LDA.

The frequency information available from the hot wire was processed by conventional spectral analysis. The shape and scaling of one-dimensional time spectra of streamwise velocity in the near-wall region of the separated zone was compared with that of the unseparated, upstream boundary layer. Of special interest is the portion of the frequency spectrum with a slope of -1 when the energy density $E(f)$ is plotted against the frequency f . This portion of the spectrum has been identified with the interaction of the mean field and the turbulence (see Ref. 21). Because of the importance of this interaction in the near-wall region, it is common practice (e.g., Ref. 22) to plot the product $f^*E(f)$ against frequency, since the interaction region shows up as a spectral peak in these coordinates.

Wall shear-stress measurements were performed using the pulsed-wall probe.¹¹ This three-wire probe is based on the conventional pulsed-wire probe, but with the three wires parallel to each other and the wall. Its performance does not

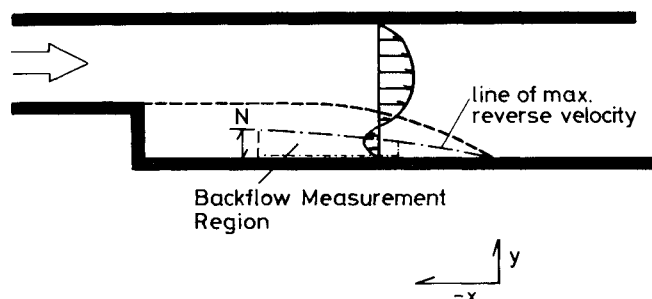


Fig. 1 Schematic of the test section showing the measurement region.

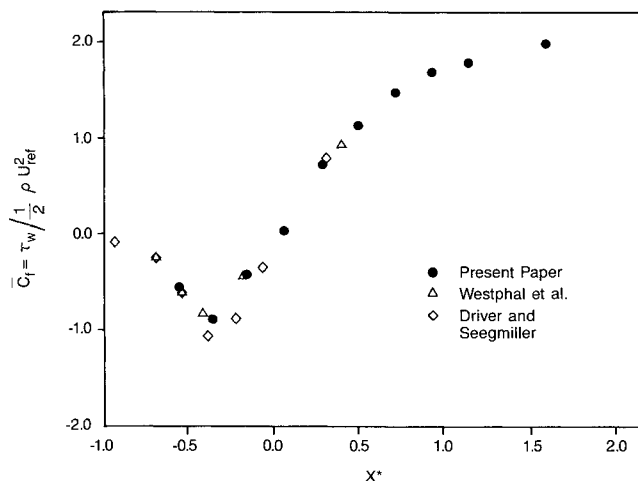


Fig. 2 Comparison of $\overline{C_\tau}$ data among several experiments; wall stress normalized on $\rho U_{ref}^2/2$, the upstream dynamic pressure.

depend upon the existence of a universal wall-layer region with a log-layer behavior.

To obtain very-near-wall streamwise velocity data with the LDA, the step-side wall was bowed vertically across its span along the streamwise centerline of the duct. This permitted the beam intersection region, the measurement volume, to be placed as close to the wall as $0.03 H$ (1 mm). The maximum upward shift of the wall at the centerline was small, about 0.05 – $0.1 H$. This bowing of the wall caused a change in step height, and thus the reattachment point changed from $6.4 H$ for the nominal flat-wall condition to $6.0 H$ for the bowed condition, where H is the step height with a flat step-side wall. However, when results from flat and bowed conditions are compared, they are virtually identical if the normalized X^* coordinate is based on the reattachment distance for the respective condition. In addition, wall shear stress profiles with X^* normalized in this fashion are relatively independent of expansion ratio for the small changes in ER (from 1.25 to ~ 1.24) created in our experiments. This demonstrated that the bowed-wall LDA measurements could be used together with wall stress measurements taken on the unbowed test surface.

Results

The wall-shear-stress data for the separated region are shown in Fig. 2 along with the results of Westphal et al.¹³ and Driver and Seegmiller.¹⁰ Westphal¹³ used the same wall shear probe as the present authors, while Driver and Seegmiller used laser interferometry to measure the rate of change of thickness of an oil drop on the wall to find the local mean shear stress. The good agreement between the two methods when plotted on $-X^*$ gives good confidence in the measurement technique used here. In addition, although all of the data presented had a turbulent inlet boundary layer at the step edge, the expansion ratios and Reynolds numbers of the three experiments differed rather widely. Thus, the observed collapse of normalized wall shear-stress coefficient \bar{C}_f vs X^* for turbulent boundary-layer inlet conditions may be a general result. Skin-friction coefficients can be defined two ways: as $\bar{C}_f = 2\tau_w/\rho U_{ref}^2$ and as the local value $C_f = 2\tau_w/\rho U_N^2$; C_f vs X^* may be Reynolds number dependent (see Ref. 12), but for turbulent layers at separation, \bar{C}_f appears to lack Reynolds number dependence.

The wall-pressure distribution in the backflow region for the present experiment is shown in Fig. 3. In $-X^*$ coordinates, the near-wall region is accelerated by the favorable pressure gradient away from the reattachment point $-X^* = 0$ toward the step. Downstream of $-X^* = 0.6$, the pressure gradient is slightly adverse. This adverse pressure gradient, of

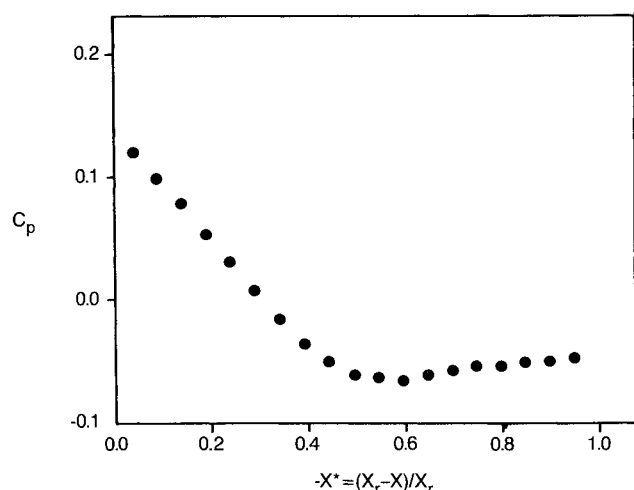


Fig. 3 Backflow region pressure distribution: $Re_H = 36,000$, $\delta/H = 1.0$; reattachment is at $-X^* = 0$; $C_p = 2(p - p_{ref})/\rho U_{ref}^2$.

course, is due to the stagnation point created as the reverse flow hits the step and results in the reattachment just ahead of the step close to $-X^* = 0.9$.

The distribution of maximum backflow velocity U_N in the separation zone is shown in Fig. 4. Here, the results from the preliminary LDA experiments along with those of the bowed-wall LDA experiments are combined with the hot-wire results and the results of Eaton and Johnston,¹⁴ who used a pulsed-wire anemometer. Again, the data collapse reasonably in $-X^*$ coordinates, even though the data of Ref. 14 are for a backward-facing step of expansion ratio 1.67, not 1.25. The maximum velocity measured by the LDA is in agreement with the hot-wire data to within the uncertainty of the data. The streamwise development of the velocity in the favorable pressure-gradient region roughly follows the power-law relationship $U_N = C^m$, where m has a value between 0.5 and 1.0 (see line in Fig. 4).

The data of Fig. 4 can be used to calculate the acceleration parameter $K = (v/U_N^2)(dU_N/dx)$ used in studies of turbulent wall layers with strong streamwise acceleration and relaminarization. In the present case with $m = 0.7$, the value of K is approximately 1.0×10^{-4} , two orders of magnitude larger than the accepted relaminarization limit 3.0×10^{-6} . Such a

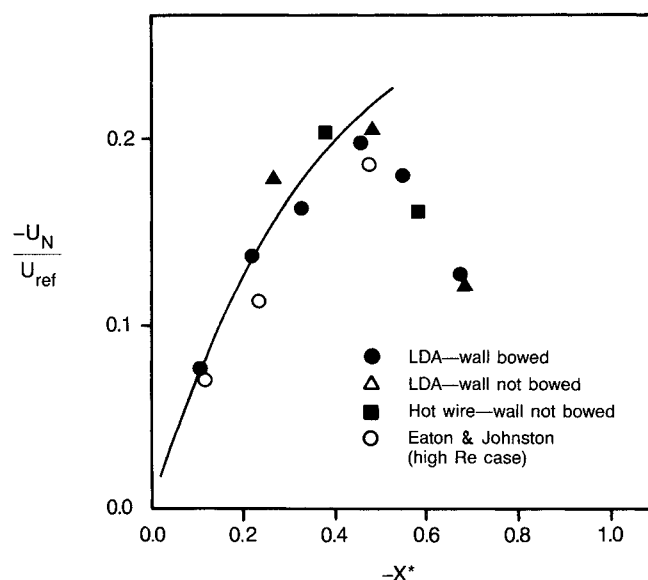


Fig. 4 Distribution of maximum reverse-flow velocity in the recirculation region.

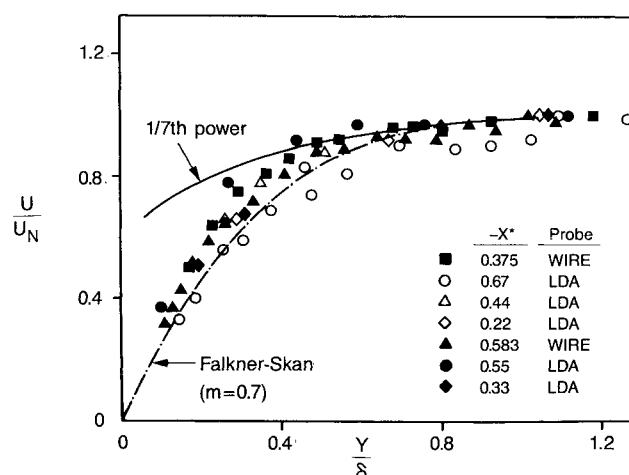


Fig. 5 Mean velocity profiles in the near-wall region compared with typical laminar and turbulent profiles.

strong streamwise acceleration must have a very strong stabilizing effect on this shear layer, over $-X^* = 0-0.5$.

The normalized velocity profiles for the near-wall region of the separation zone are shown in Fig. 5. The pressure gradient associated with these profiles is strongly favorable for $-X^* < 0.5$ and mildly adverse for $-X^* > 0.5$. For comparison purposes, Fig. 5 also shows a one-seventh power-law profile and a Falkner-Skan profile for $m = 0.7$. The shape of the data fits that of the Falkner-Skan profile much better than the one-seventh law profile. The large near-wall gradient of $\partial u / \partial y$, which controls the typical shape of a normal turbulent profile, results from momentum exchange obtained from the turbulent $-\overline{u'v'}$ component of shear stress in the near-wall region. The rounder, full shape of the data is an indication that the effective Reynolds number of the flow is quite low and that the Reynolds shear stress $-\overline{u'v'}$ is not playing a major role in near-wall momentum exchange. Although there is some scatter in the data of Fig. 5, it was impossible, by changing the value of δ_{99} , to change the basic shape of the profile from that of the Falkner-Skan solutions to the one-seventh law profile. (First, a wide variety of pressure gradients exists between the step and reattachment; thus, in these coordinates, a full collapse would be surprising. Second, the definition of $N = \delta$ is subject to about a 10% error, and this leads to some scatter.)

Using u_r from the pulsed-wall probe data to obtain $U^+ = U/u_r$, near-wall velocity profiles were plotted in wall coordinates (see Fig. 6). All the data on the figure lie far below the turbulent log-law. In most cases, δ lies between 40 and 100 wall units away from the wall, making the layer "too thin" to have a well-developed log region. This is also an indication that viscous forces are more important than the Reynolds shear stresses in this shear layer. Figure 6 also shows a sample U^+, Y^+ profile of Ruderich and Fernholz⁹ for the flow on a splitter plate behind a plate normal to the flow. This high Reynolds number separated and reattaching flow results from a different but related geometry; the log-law does not hold here either. Similar trends are seen in Devenport's results.⁸ The absence of a log-law region under separated flows seems a rather general result. Figure 6 also suggests that there is no mean profile similarity anywhere above $Y^+ = 10$.

Near $Y^+ = 1$, the data must approach the profile ($U^+ = Y^+$) shown on the plot. However, not all of the profiles show smooth behavior in this region. The scatter of the data inside $Y^+ = 10$ is due to a combination of errors in the velocity and measuring volume position measurement. The uncertainty due to the position measurement is probably the largest, being about two wall units for the LDA and somewhat less for the hot wire.

By treating each profile in the near-wall region as a boundary-layer profile, boundary-layer integral parameters may be identified. The nearly linear streamwise development

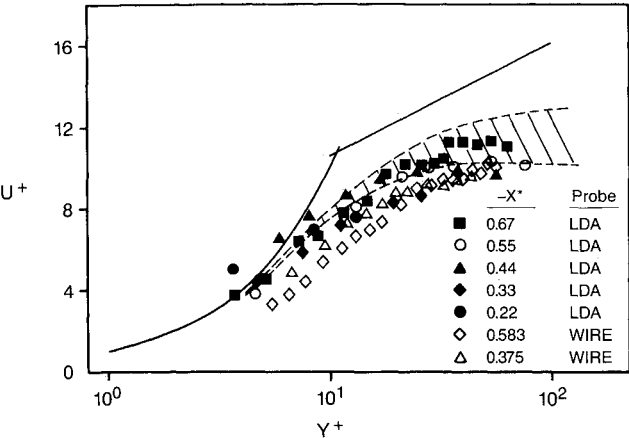


Fig. 6 Mean velocity in the near-wall region in log coordinates; shaded region is the data of Ruderich and Fernholz.⁹

Table 1 Reynolds numbers of the near-wall region					
$-X^*$	X/H	Re_N	Re_θ	Re_{δ^*}	$Re_{\delta_{99}}$
0.67	4.67	98	12	25	97
0.55	4.00	219	25	53	210
0.44	3.33	362	25	53	229
0.33	2.67	543	45	95	498
0.22	2.0	372	55	96	372

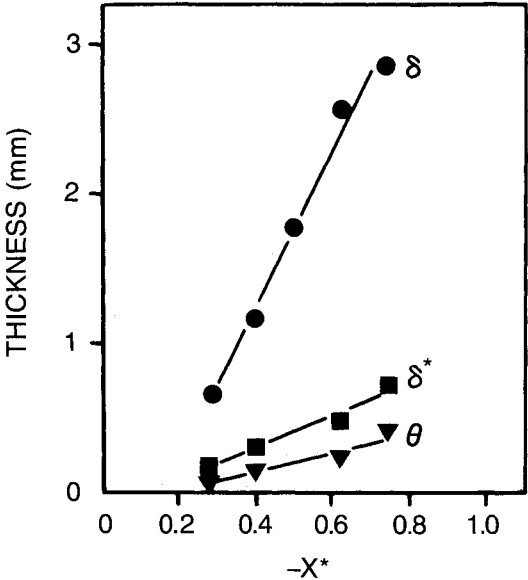


Fig. 7 Boundary-layer thickness and integral parameters in the near-wall region of the recirculation zone.

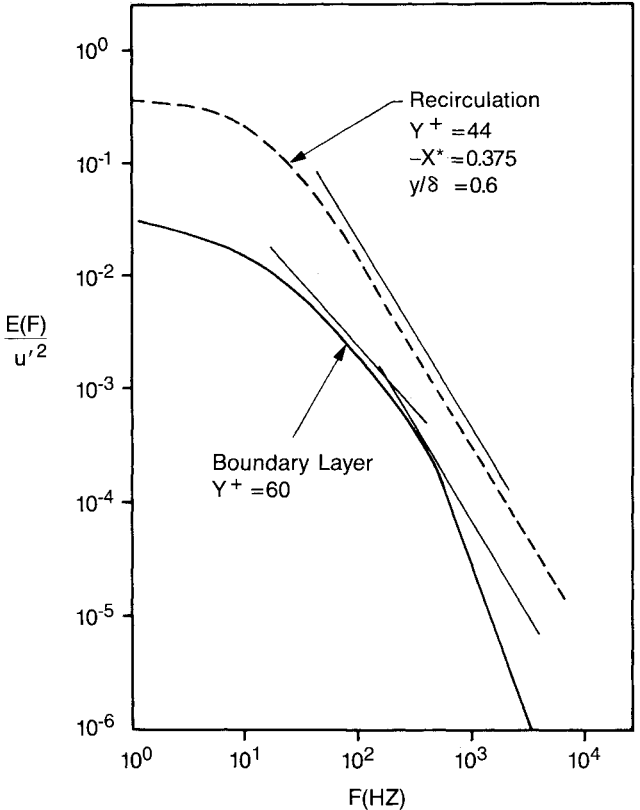


Fig. 8 Comparison of frequency spectra between the very-near-wall region of the recirculation zone and the upstream boundary layer; slopes shown are -1 and $-5/3$.

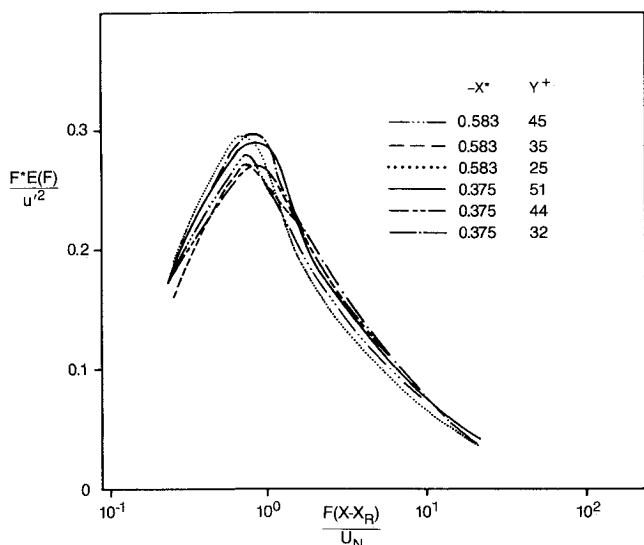


Fig. 9 Collapse of spectral shapes for $Y^+ > 10$ in the recirculation region.

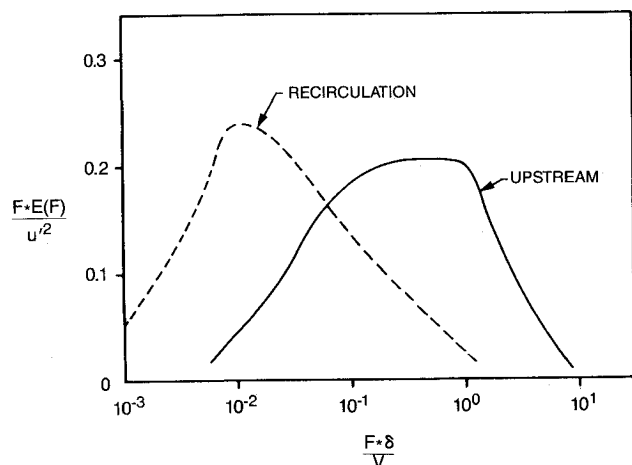


Fig. 10 Comparison of outer-region scaling between the upstream boundary layer and the recirculation region at constant distance from the wall: $y/H = 0.043$, $-X^* = 0.375$.

of the integral parameters is shown in Fig. 7. The value of the shape factor $H = \delta^*/\theta$, calculated from the integral parameters of Fig. 7, is approximately 2.05 throughout the measurement region. The nearly constant value of H , despite pressure gradient differences, indicates that the velocity data cannot be explained by pressure gradient effects alone. A linear development of the integral parameters is not associated with laminar boundary layers. This is a clear indication that, although many features of the near-wall shear layer more closely resemble a LBL than a TBL, this viscous region may be laminar-like but not laminar.

The magnitudes of various boundary-layer Reynolds numbers for the wall layer are shown in Table 1. The small magnitudes of these Reynolds numbers confirm the speculation of Westphal¹³ that Re_N is roughly 50 times smaller than Re_H . The maximum Re_θ is 50, and the boundary-layer-thickness Reynolds number is at most 500, while the Reynolds number based on streamwise distance from reattachment is at most 20,000. These local Reynolds numbers suggest that disturbances are damped in this layer and that they are consistent with the lack of a log-law region and the shape of

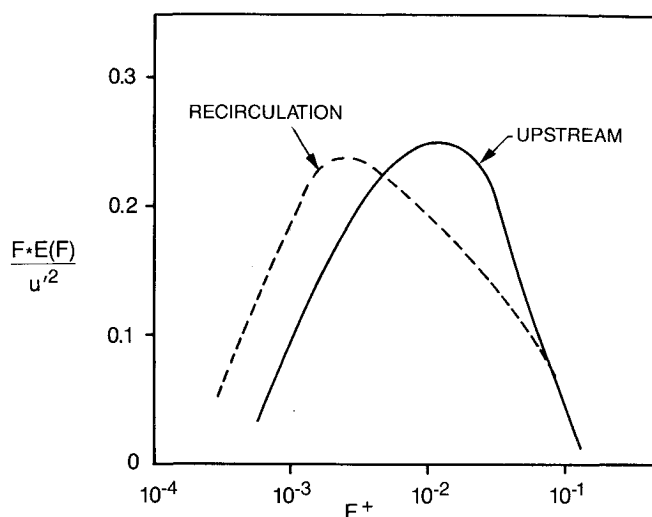


Fig. 11 Comparison of inner scaling between the recirculation region and the upstream boundary layer at $Y^+ = 25$.

the velocity profiles given in Fig. 5. This is simply too viscous to develop the typical features of turbulent wall layers.

Figure 8 presents two one-dimensional spectra of the streamwise velocity, one obtained in the upstream boundary layer and the other in the recirculation zone. The spectra from the backflow zone, with Y^+ greater than 20, show a much longer inertial subrange ($-5/3$ slope region) than those taken in the upstream boundary layer. A larger inertial subrange is usually indicative of a higher turbulence Reynolds number $u'\ell/\nu$ (see Ref. 23). Thus, while the Reynolds numbers for the near-wall shear layer based on mean quantities are quite low, the effective Reynolds number of the turbulence field appears to be quite large. This inconsistency suggests that the descriptive Reynolds number of the turbulence field is different from the descriptive Reynolds number of the mean flowfield. This is possible if, as proposed by Simpson et al.,⁶ the large, normal, turbulent stresses are not generated locally near the wall but in the free shear layer or at reattachment.

The non-normalized spectral data from the near-wall region had substantial low-frequency content. At $-X^* = 0.583$, the spectral "peak" when the spectra are plotted as $f^*E(f)/u'^2$ vs f occurred at 10 Hz, while at $-X^* = 0.38$, the spectral peak occurred at 30 Hz. These low frequencies suggested that the turbulence fluctuations are dominated by processes that scale on the size of the separation bubble itself. Figure 9 shows these data using a new frequency scaling. The data collapse as indicated if frequency is nondimensionalized using streamwise distance from the reattachment point and the local, maximum, reverse-flow velocity U_N . A scaling $f^* = f(x_r - x)/U_N$ results. This scaling suggests that the global processes associated with the free shear layer and separation bubble dominate over the near-wall processes in the backflow zone for the determination of levels of u' . Other scalings tried without success were the following: 1) length based on height from the wall to the dividing streamline and either the velocity on the dividing streamline or the local velocity, and 2) length of the entire separation bubble and local velocity.

Our results may be compared to those of Simpson et al.,⁶ who also measured some spectral peaks. In the present flow, dominant frequencies of the streamwise velocity fluctuations were found to scale on the distance from the reattachment point. Simpson's frequencies ranged from $f d/U_\infty = 10$ –20 for the region above $y = 0.5 N$. If these frequencies are rescaled on distance from separation, a parameter $f(x - x_s)/U_N$ is formed. Its value is 0.5–1.0, in nice agreement with the results shown in Fig. 9.

The wall-layer thickness N could also be used as the length scale and the data would collapse, but fN/U_N would take the

value 0.01, not as satisfactory physically, since it suggests that the eddy size is on the order of $100 N$. By contrast, the scaling $f(x - x_s)/U_N$ suggests that the eddies are of the same extent as the distance to separation (or reattachment), a plausible size. Such large eddies are consistent with the high levels of diffusion measured by Simpson et al.⁶ and by Pronchick and Kline.¹⁵

Spectra from the backflow region and from the upstream boundary layer were compared using conventional inner and outer scaling in Figs. 10 and 11. Outer scaling was compared at constant distance from the wall (Fig. 12). The spectra taken in the upstream TBL agree qualitatively with the results of Perry and Abell²⁴ and of Johansson and Alfredsson,²² who present data at different values of Y^+ . The location of the spectral peak in the recirculation region is two decades lower than that of the upstream boundary layer when outer scaling is used. Because Perry and Abell²⁴ have shown that increasing distance from the wall leads to increasing rather than decreasing frequency, a comparison at constant y/δ_{99} would result in even greater disagreement between the upstream boundary layer and the wall layer in the backflow zone.

Inner scaling laws applied to streamwise velocity spectra were compared at similar Y^+ values. At $Y^+ = 25$ (see Fig. 11), there is no collapse of the data in any frequency range. The locations of the spectral peaks in this normalization differ by a factor of 6–10, well outside any uncertainty arising from uncertainty in the values of u_r .

Figures 12 and 13 present one-dimensional frequency spectra in the upstream boundary layer and the separation zone, respectively. In the upstream TBL, the near-wall spectra are largely independent of position normal to the wall. Figure 12 illustrates this for Y^+ values of 9 and 25. While Perry and Abell²⁴ noted differences in spectral shape below $Y^+ = 100$, their data also show no major movement of the spectral peak. Bakewell and Lumley²⁵ have measured very-near-wall spectra in normal attached flow in which the frequency content did not change with Y^+ location when normalized in this fashion. This result is expected if the bursting process is dominating the near-wall spectral content. Figure 12 may be contrasted to the results for the near-wall region in the recirculation zone shown in Fig. 13. Here, differences in the spectral behavior with distance from the wall are noted for spectra from the recirculation zone. The spectra show increasing levels of high-frequency content as the wall is approached.

In light of the mean velocity results and the fact that the spectra of the turbulence in the recirculation region scale on the distance from reattachment and not on boundary-layer parameters, it is hardly surprising that large differences exist in the behavior of the turbulence spectra as the wall is

approached between the near-wall region of a separated flow and a normal turbulent boundary layer. The spectra shown in Fig. 13 for the near-wall region of the separation zone display behavior similar to that of a Stokes layer subjected to a broad band of freestream fluctuation frequencies. Compared to the high frequencies, lower frequencies are damped faster as the wall is approached.

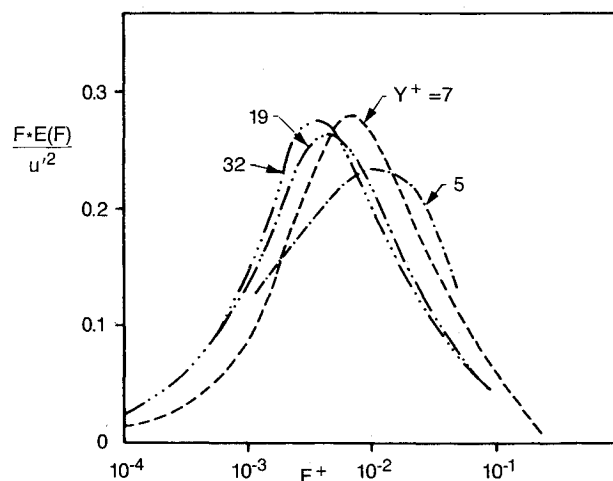


Fig. 13 The effect of wall proximity on the spectral shapes in the recirculation zone.

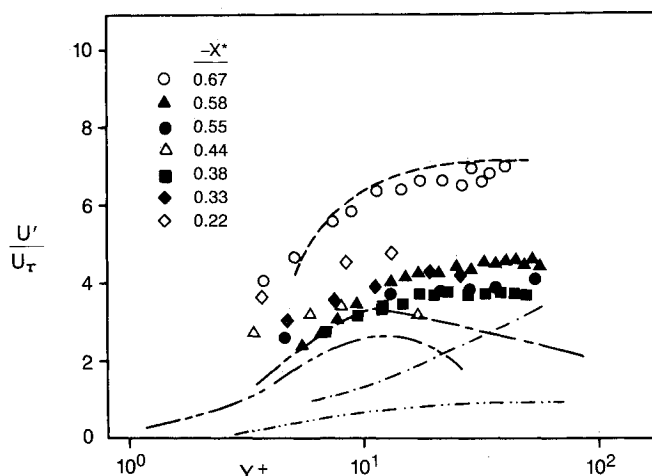


Fig. 14 Near-wall profiles of fluctuation velocity in the recirculation zone: — u' Simpson et al.,⁶ separated layer; - - v' Simpson et al.,⁶ separated layer; — u' Laufer,²⁶ turbulent pipe flow; - - v' Laufer,²⁶ turbulent pipe flow; — u' Eckelmann,²⁷ boundary layer.

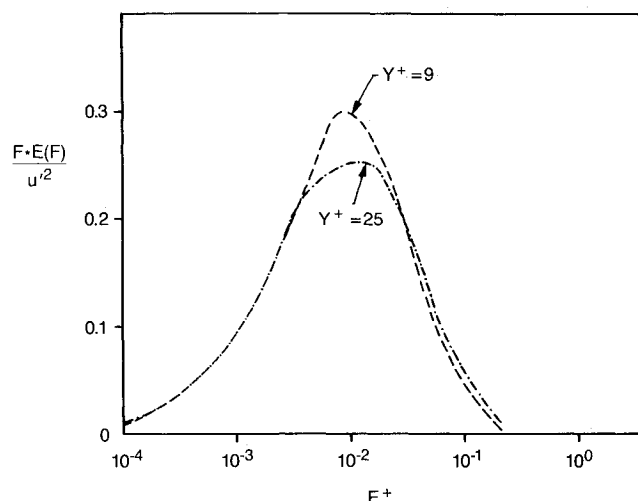


Fig. 12 The effect of wall proximity on the spectral shapes in the upstream boundary layer.

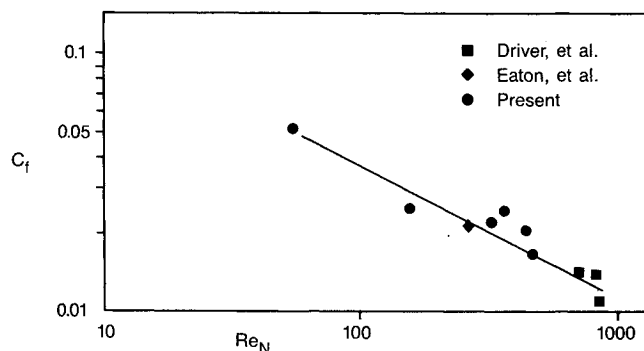


Fig. 15 Comparison of all known wall-skin-friction data in the recirculation zone as a function of wall-layer Reynolds number; line shown has a slope of $-1/2$; $C_f = 2\tau_w/\rho U_N^2$.

The rms fluctuation level of streamwise velocity for several locations is shown in Fig. 14. Also shown in the figure are the u' and v' data of others for separated and normal TBL conditions. Simpson⁶ did not measure u_r ; therefore, to produce the wall-layer normalization, the value of u_r was estimated here by setting $U^+ = Y^+$ at the data point nearest the wall. (Figure 6 suggests that the value of u_r obtained in this manner will be 10–20% too low, since the first point is close to $Y^+ = 5.0$.) The values of u'/u_r vary widely because u_r is not the best parameter for normalizing u' ; peak $(\overline{u'v'})^{0.5}$ or peak u' in the shear layer would be better. Despite this small difficulty, the data in Fig. 14 are useful. The unseparated flow profiles from Refs. 26 and 27 attain peak levels between $Y^+ = 10$ and 20. This peak is associated with the region of maximum TKE production. The absence of a peak in the present data, as well as in Simpson's data, suggests that the production process is different from that in a normal, unseparated TBL.

Discussion

The results in the previous section suggest that modeling the near-wall layer of a separation bubble as a normal turbulent boundary layer (albeit flowing backwards) is not correct. For example, the mean velocity profiles do not follow the "law of the wall." Although many features of the mean flow results for this highly viscous layer closely resemble results for laminar boundary layers, the layer is not laminar, since there are very high fluctuation levels in this region. This layer is viscous dominated, however unsteady it may be.

It is suggested as a model of these data that the flow is so dominated by viscous effects that the Reynolds shear stress is relatively unimportant and the mean flow can be considered to be uncoupled from the turbulence. A viscous model of the mean flow suggests a velocity profile law of the type $U/U_N = f(Y, N, \nu)$ if it is assumed that only the parameters U_N , N , and ν affect the flow structure. The wall shear must be a function of Re_N alone. Such an assumption does seem to be validated by the C_f data plotted in Fig. 15. Also shown are other back-step results^{10,14} at all locations where both U_N and C_f could be defined. Considering the wide variety of Reynolds numbers and expansion ratios between these experiments, the collapse of all data to a $-1/2$ slope is rather surprising. Using $1/2$ power-law scaling, $y^* = y \sqrt{U_N/N\nu}$, the mean velocity data $u^* = U/U_N$ should collapse, and it appears to do so in Fig. 16. It should be noted, though, that true wall-layer similarity would be rather surprising because of the range of pressure gradients encountered in this region.

If the effect of the Reynolds stresses on the mean motion dynamics is to be small, the shear-stress gradient $d(-\overline{u'v'})/dy$ must also be small. Measurements by others show $-\overline{u'v'}$ to be small throughout the near-wall zone, implying a small value of the gradient. Despite the low values of $-\overline{u'v'}$, the near-wall magnitudes of the normal stresses u'^2 are similar to levels in turbulent boundary layers. The reason why the normal stresses do not give rise to shear-stress generation, as in normal TBL's, can be seen by considering the production terms in the partial differential equations for the Reynolds stresses:

$$P(\overline{u'^2}) = -2\overline{u'^2} \frac{\partial U}{\partial x} + \overline{u'v'} \frac{\partial U}{\partial y}$$

$$P(\overline{v'^2}) = -2\overline{v'^2} \frac{\partial V}{\partial y}$$

$$P(\overline{u'v'}) = -\overline{v'^2} \frac{\partial U}{\partial y}$$

Figures 5 and 6 show that for $Y^+ = 5$ the mean-velocity gradient is much smaller than in a normal TBL. Consequently, the $\partial U/\partial y$ production terms are also smaller. Without the production of $\overline{u'^2}$ associated with $\rho \overline{u'v'}$, a peak in the u' profiles can't exist close to the wall (see Fig. 14).

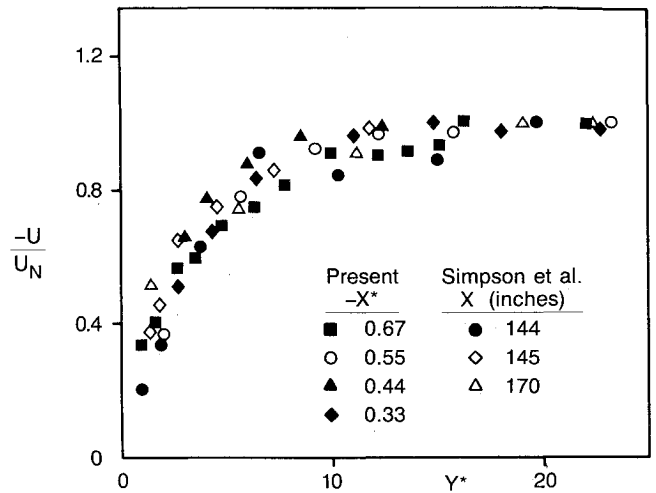


Fig. 16 New mean velocity scaling for the near-wall region of separated flows, $y^* = y \sqrt{U_N/\nu N}$.

In normal TBL's, the spectral peak that relates the interaction of the mean flow and the turbulence scales on variables typical of the important eddy frequencies associated with the local production of turbulence. In the highly viscous near-wall layer, there is almost no production, and hence local scaling fails. The successful scaling of the frequencies of the spectra using $(x_R - x)$ and U_N indicates that the turbulence found in the near-wall region is produced by the large eddies in the recirculation region—above and not in this near-wall layer. Finally, the shift of the spectral content to higher frequencies as the wall is approached and the character of the turbulence profiles is consistent with the viscous damping, which would occur in this near-wall region without significant $-\rho \overline{u'v'}$.

The close agreement between the spectral data of Simpson et al.⁶ in a separated diffuser and the present data is interesting. In the Simpson diffuser flow, the distance from separation is an important parameter; in the present flow it is distance from reattachment. In the backstep, mean convection is away from reattachment, while in separating flows, convection is toward separation. In the Simpson et al. flow, near-wall frequencies decrease in the downstream (away from detachment) direction, just as in the free shear layer above the near-wall zone. In the backstep flow, important frequencies in the near-wall region decrease in the upstream direction, while in the free shear layer, eddy sizes decrease and frequencies increase in the upstream direction (away from reattachment). Despite these differences, the turbulence structures in these two types of flows are clearly related. The correspondence of the energy-balance data of Simpson et al.⁶ in separating flows and data of Pronchick and Kline¹⁵ for backsteps also indicates the close relationship between these two flows of vastly different geometry.

Conclusions

All measurements reported herein suggest that the structure of the near-wall region of a separated flow is different from that of a normal turbulent boundary layer:

- 1) There is no standard logarithmic region in the present flow.
- 2) Skin-friction and velocity-profile results suggest a highly viscous mean flow in which the role of the turbulent shear stresses is minor compared to that of their laminar counterparts.
- 3) Frequency spectra scale on $(x_r - x)$ and U_N rather than on local variables.

The mean flow and skin-friction scaling presented was viscous in nature and inconsistent with the appearance of a

log-law. The turbulence in the near-wall region is not generated in this region, and its structure is a combination of the features of the large eddies above the near-wall region where it was created and the damping effect of the wall. The near-wall region has a number of laminar-like features but is not laminar.

Acknowledgments

This work was supported by the Fluid Mechanics Program, Engineering Division, National Science Foundation. The authors are grateful for the support and interactions of their colleagues; in particular, Prof. J. K. Eaton, Dr. J. Vogel, Dr. A. Cutler, and Dr. R. Barlow.

References

- ¹Chapman, D. R., Kuehn, D. M., and Larson, H. K., "Investigation of Separated Flow with Emphasis on the Effect of Transition," NACA Rept. 1356, 1958.
- ²Abbott, D. E. and Kline, S. J., "Theoretical and Experimental Investigation of Flow Over Single and Double Backward-Facing Steps," Thermosciences Div., Mechanical Engineering Dept., Stanford Univ., Stanford, CA, Rept. MD-5, 1961.
- ³Bradshaw, P. and Wong, F. Y. E., "The Reattachment and Relaxation of a Turbulent Shear Layer," *Journal of Fluid Mechanics*, Vol. 52, Pt. 1, March 1972, pp. 113-135.
- ⁴Kim, J., Kline, S. J., and Johnston, J. P., "Investigation of Separation and Reattachment of a Turbulent Shear Layer: Flow Over a Backward-Facing Step," Thermosciences Div., Mechanical Engineering Dept., Stanford Univ., Stanford, CA, Rept. MD-7, April 1978.
- ⁵Mueller, T. J., "On Separation, Reattachment, and Redevelopment of Turbulent Boundary Layers," Ph.D. Dissertation, Mechanical Engineering Dept., Univ. of Illinois, Urbana, IL, 1961.
- ⁶Simpson, R. L., Chew, Y.-T., and Shivaprasad, B. G., "The Structure of a Separating Turbulent Boundary Layer. Part 1. Mean Flow and Reynolds Stresses," *Journal of Fluid Mechanics*, Vol. 113, Dec. 1981, pp. 23-51.
- ⁷Simpson, R. L., "A Model for the Backflow Mean Velocity Profile," *AIAA Journal*, Vol. 21, Jan. 1983, pp. 142-143.
- ⁸Devenport, W. J., "Separation Bubbles at High Reynolds Number: Measurement and Computation," Ph.D. Dissertation, Univ. of Cambridge, Cambridge, England, UK, 1985.
- ⁹Rudrich, R. and Fernholz, H. H., "An Experimental Investigation of a Turbulent Shear Flow with Separation, Reverse Flow, and Reattachment," *Journal of Fluid Mechanics*, Vol. 163, Feb. 1986, pp. 283-322.
- ¹⁰Driver, D. M. and Seegmiller, H. L., "Features of a Reattaching Turbulent Shear Layer in Divergent Channel Flow," *AIAA Journal*, Vol. 23, Feb. 1985, pp. 163-171.
- ¹¹Westphal, R. V., Eaton, J. K., and Johnston, J. P., "A New Probe for Measurements of Velocity and Wall Shear Stress in Unsteady, Reversing Flow," *Journal of Fluids Engineering*, Vol. 103, Sept. 1981, p. 478.
- ¹²Castro, I. P. and Haque, A., "The Structure of a Turbulent Shear Layer Bounding a Separation Region," *Journal of Fluid Mechanics*, Vol. 179, June 1987, pp. 439-468.
- ¹³Westphal, R. V., Johnston, J. P., and Eaton, J. K., "Experimental Study of Flow Reattachment in a Single-Sided Expansion," NASA CR-3765, Jan. 1984.
- ¹⁴Eaton, J. K., and Johnston, J. P., "Turbulent Flow Reattachment: An Experimental Study of the Flow and Structure Behind a Backward-Facing Step," Thermosciences Div., Mechanical Engineering Dept., Stanford Univ., Stanford, CA, Rept. MD-39, 1980.
- ¹⁵Pronchick, S. W. and Kline, S. J., "An Experimental Investigation of the Structure of a Turbulent Reattaching Flow Behind a Backward-Facing Step," Thermosciences Div., Mechanical Engineering Dept., Stanford Univ., Stanford, CA, Rept. MD-42, June 1983.
- ¹⁶Stevenson, W. H., Thompson, H. D., and Craig, R. R., "Laser Velocimeter Measurements in Highly Turbulent Recirculating Flows," *ASME Journal of Fluids Engineering*, Vol. 106, No. 2, June 1984, pp. 173-180.
- ¹⁷Adams, E. W., Johnston, J. P., and Eaton, J. K., "Experiments on the Structure of Turbulent Reattaching Flow," Thermosciences Div., Mechanical Engineering Dept., Stanford Univ., Stanford, CA, Rept. MD-43, 1984.
- ¹⁸Brederode, V. and Bradshaw, P., "Three-Dimensional Flow in Nominally Two-Dimensional Separation Bubbles. I. Flow Behind a Rearward-Facing Step," Imperial College of Science and Technology, London, England, I. C. Aero Rept. 72-19, 1972.
- ¹⁹Adams, E. W. and Eaton, J. K., "An LDA Study of the Backward-Facing Step Flow Including the Effects of Velocity Bias," *Proceedings of the ASME Winter Annual Meeting*, Vol. FED 33, American Society of Mechanical Engineers, New York, 1985, pp. 255-264.
- ²⁰Kline, S. J., Sovran, G., Morkovin, M. V., and Cockrell, D. J., *Proceedings, Computation of Turbulent Boundary Layers—1968 AFOSR-IFP-Stanford Conference*, Thermosciences Div., Mechanical Engineering Dept., Stanford Univ., Stanford, CA, 1968.
- ²¹Tchen, C. M., "On the Spectrum of Energy in Turbulent Shear Flow," *Journal of Research*, National Bureau of Standards, Vol. 50, 1953, p. 51.
- ²²Johansson, A. V. and Alfredsson, P. H., "On the Structure of Turbulent Channel Flow," *Journal of Fluid Mechanics*, Vol. 122, Sept. 1982, pp. 295-314.
- ²³Tennekes, H. and Lumley, T. L., *A First Course in Turbulence*, MIT Press, Cambridge, MA, 1972.
- ²⁴Perry, A. E. and Abell, C. J., "Scaling Laws for Pipe-Flow Turbulence," *Journal of Fluid Mechanics*, Vol. 67, Pt. 2, Jan. 1975, pp. 257-271.
- ²⁵Bakewell, H. P., Jr. and Lumley, J. L., "Viscous Sublayer and Adjacent Wall Region in Turbulent Pipe Flow," *Physics of Fluids*, Vol. 10, Sept. 1967, pp. 1880-1889.
- ²⁶Lauffer, J., "The Structure of Turbulence in Fully Developed Pipe Flow," NACA Tech. Rept. 1174, 1954.
- ²⁷Kreplin, H.-P. and Eckelmann, H., "Behavior of the Three Fluctuating Velocity Components in the Wall Region of a Turbulent Channel Flow," *Physics of Fluids*, Vol. 41, No. 7, July 1979, p. 1233.